Published on 15 November 2016. Downloaded by Polska Akademia Nauk Instytut Chemii Fizycznej on 02/03/2017 17:06:29.

Analytical Methods

PAPER

View Article Online
View Journal | View Issue

Cite this: *Anal. Methods*, 2016, **8**, 8427

Detection and identification of human fungal pathogens using surface-enhanced Raman spectroscopy and principal component analysis†

Evelin Witkowska,[a] Tomasz Jagielski,[b] Agnieszka Kamińska,*[a] Aneta Kowalska,[a] Anita Hryncewicz-Gwóźdź[d] and Jacek Waluk[ac]

This paper demonstrates that surface-enhanced Raman spectroscopy (SERS) coupled with principal component analysis (PCA) can serve as a fast and reliable technique for the detection and identification of human fungal pathogens, such as *Trichophyton rubrum*, *Candida krusei*, *Scopulariopsis brumptii*, and *Aspergillus flavus*. Fungal infections have become one of the leading infectious causes of morbidity and mortality among hospitalized patients and/or immunocompromised hosts. Hence, there is a strong need for the development of new technologies allowing for fast and reliable diagnosis of fungal diseases. Our study shows that the SERS technique effectively distinguishes between selected common fungal pathogens and thus offers taxonomic affiliation of fungi within several minutes. Additionally, the PCA analysis allows performing statistical classification of fungal pathogens studied and identifying the fungal spectrum directly from a clinical sample. Calculated two principal components (PCs) (PC-1, PC-2) are the most diagnostically significant, explain 97% of the variability and enable, with very high probability, discrimination between the four mentioned fungal species. Moreover, the results of this study demonstrate the excellent possibility for the identification of fungi from human skin samples. The research presented in this paper offers an alternative for conventional fungal diagnostics and paves the way for the development of a new, fast, robust, and cost-effective diagnostic test for the detection and identification of fungal pathogens.

Received 28th October 2016
Accepted 11th November 2016

DOI: 10.1039/c6ay02957d

www.rsc.org/methods

1. Introduction

There are approximately 1.5 million different species of fungi on Earth,[1] of which less than 300 species are known to cause infections in humans and animals.[2] Fungal diseases or mycoses are often caused by species that are widely distributed in the environment. Most of these organisms are normally saprotrophs inhabiting soil, water, or vegetation and only in certain instances do they switch into pathogenic mode and cause a disease, which clinically may range from mild through moderate to severe with death occasionally occurring. Only a few species are relatively common pathogens and have been responsible for the bulk of human infections. Disturbingly, the prevalence of fungal infections has been on the rise in recent years, and this has been attributed to a rapidly expanding population of immunocompromised patients, increased rates of invasive treatment options, such as surgery, multidrug chemotherapy, irradiation, and the widespread use of antibiotics and other antimicrobial agents.[3,4] Since fungi are the most common cause of morbidity and mortality among immunocompromised patients,[5] diagnosis and management of fungal infections still pose a great challenge to health care professionals.

Conventional identification of fungi is phenotype-based and involves morphological and metabolic characterization. The time required to culture an isolate from a clinical sample may exceed 2 months. Although yeasts usually grow within 24–72 hours, for dermatophytes even a 4 week incubation period is necessary.[6] Along with macro/micromorphological studies and biochemical testing of cultured isolates, diagnosis can be assisted by serological profiling and pathological examination of the biopsy specimen.[7,8] A very useful adjunct to the diagnostic algorithm of fungal infections is molecular typing. A wide array of fast and simple nucleic acid-based tests have been proposed. Most of these assays follow the same general pattern, *i.e.* (i) extraction of genomic DNA, (ii) PCR-based amplification of a selected region of the genome, most often within the rDNA cluster, and

[a]*Institute of Physical Chemistry, Polish Academy of Sciences, Kasprzaka 44/52, 01-224 Warsaw, Poland. E-mail: akamin@ichf.edu.pl*

[b]*University of Warsaw, Faculty of Biology, Institute of Microbiology, Department of Applied Microbiology, I. Miecznikowa 1, 02-096 Warsaw, Poland*

[c]*Faculty of Mathematics and Natural Sciences, College of Science, Cardinal Stefan Wyszyński University, Dewajtis 5, 01-815 Warsaw, Poland*

[d]*Wrocław Medical University, Department of Dermatology, Venereology and Allergology, T. Chałubińskiego 1, 50-368 Wrocław, Poland*

† Electronic supplementary information (ESI) available. See DOI: 10.1039/c6ay02957d

Published on 15 November 2016. Downloaded by Polska Akademia Nauk Instytut Chemii Fizycznej on 02/03/2017 17:06:29.

(iii) analysis of the resulting PCR product, usually by probe hybridization or DNA sequencing.[9,10]

Neither of the methods currently used for the detection and identification of fungal pathogens is optimal. Each has its strengths and weaknesses. While searching for an ideal diagnostic option, not only analytical criteria, such as resolution or differentiation capacity, accuracy and reproducibility have to be considered, but also some practicalities, including time and cost of analysis, ease of performance or equipment and personnel demands of the method.

In this work we present a novel, fast and simple method for the detection and identification of selected human pathogenic fungi. The method exploits surface-enhanced Raman spectroscopy (SERS), whose principle was first described in the mid-1970s.[11] The SERS imaging of fungi has so far been documented only in a few reports, all devoted to single species only.[12,13] Although SERS has already been used for the identification of clinically important bacteria[14–18] and viruses,[19,20] never before has it been employed for the detection or identification of pathogenic fungi.

Our study was performed on fungi representing four different species, namely *Aspergillus flavus*, *Trichophyton rubrum*, *Scopulariopsis brumptii*, and *Candida krusei*. All these species have been implicated in human disease. *Aspergillus flavus* is one of the main agents of human allergic bronchial aspergillosis, but may also cause mycotic otitis and sinusitis.[21] *Trichophyton rubrum* is the most common dermatophyte, accounting for the majority of all superficial fungal infections in humans.[22] *Scopulariopsis brumptii*, a dematiaceous mould, has been reported as the etiologic agent of human onychomycosis[23] and sporadically invasive infections in seriously immunosuppressed patients.[24,25] Finally, *C. krusei*, a budding yeast, which, although rarely causes human infections, is the only *Candida* species inherently resistant to fluconazole, one of the primary drugs used to treat candidiasis.[26]

Surface-enhanced Raman spectroscopy (SERS) is a very promising technique for biomedical applications in whole organism fingerprint study. In the SERS technique we observe the enhancement of the Raman signal from molecules which are in close proximity to a nanostructured surface due to the coupling of metal surface plasmons with the oscillating electric field of the incident and scattered radiation. The enhancement of the Raman signal is a product of two contributions: (i) an electromagnetic enhancement mechanism, and (ii) a chemical enhancement mechanism.[27] The electromagnetic enhancement results from the amplification of light by the excitation of localized surface plasmon resonances (LSPRs). This light concentration occurs preferentially in the nanogaps or sharp nanofeatures of plasmonic materials (*e.g.*, silver, gold, and copper). Reproducible and robust structures that strongly enhance the electromagnetic field are most desirable for SERS. Depending on the structure of the supporting plasmonic material, electromagnetic enhancement for SERS is theoretically estimated to reach factors of *ca.* 10^{10} to 10^{11}. In most circumstances the enhancement factor can be well approximated by the magnitude of the localized electromagnetic field raised to the fourth power. In turn, the chemical enhancement involves charge transfer mechanisms, where the excitation wavelength is resonant with the metal-molecule charge transfer electronic states. The development of SERS substrates with high enhancement factors remains an active area of SERS research.[28]

In this paper, we present the possibility of differentiation and identification of pathogenic fungi in a label-free and fast manner using the SERS technique. Since the topic has been very poorly described in the literature, we decided to measure not only the SERS signals from fungal organisms but also the Raman signals generated by major constituents of the fungal cell wall, namely chitin, galactomannan, and β-1,3-glucan.[29] This was done to verify the origin of the signals in the fungi-derived spectra. Moreover, here we combine SERS data with the multivariate statistical methods. To show the significant spectral differences among SERS spectral features, the principal component analysis (PCA) as one of the most robust statistical methods was applied to: (i) extract biochemical information from fungal spectra, (ii) to perform the statistical classification of these microorganisms, and finally (iii) to identify the fungal spectra from clinical samples.

2. Materials and methods

2.1. Chemicals and materials

Four strains representing different fungal species, *i.e. A. flavus* (ATCC 204304), *T. rubrum*, *S. brumptii* (CBS 345.58), and *C. krusei* (DBVPG 7235 = ATCC 749) were included in the study. The strains, housed by the Department of Applied Microbiology, University of Warsaw, Poland, were originally either purchased from the Centraalbureau voor Schimmelcultures (CBS; Utrecht, the Netherlands) and from the American Type Culture Collection (ATCC; Manassas, USA) or kindly provided by collaborating laboratories.

Chitin, galactomannan and β-1,3-glucan were purchased from Sigma-Aldrich, Poland. The chemicals were used without any further purification.

Sampling of the patients was performed in accordance with the regulations and approval of the Ethics Committee of the Wrocław Medical University, Wrocław, Poland. Informed consent was obtained from all patients.

2.2. Instrumentation

SERS measurements were performed using a Renishaw inVia Raman system equipped with a 300 mW diode laser emitting a 785 nm line which was used as an excitation source. The laser light was passed through a line filter and focused on a sample mounted on an X–Y–Z translation stage with a 50× objective lens (numerical aperture 0.75) that focused the laser to a spot size of around 2.5 μm. The Raman-scattered light was collected by the same objective through a holographic notch filter to block the Rayleigh scattering. A 1200 grooves per mm grating was used to provide a spectral resolution of 5 cm^{-1}. The Raman scattering signal was recorded by using a 1024 × 256 pixel RenCam CCD detector. Typically, 30 SERS spectra of studied fungal cells were acquired for 60 s, with 5 mW of the laser power measured at the sample. For clinical skin sample measurement

 This journal is © The Royal Society of Chemistry 2016

Published on 15 November 2016. Downloaded by Polska Akademia Nauk Instytut Chemii Fizycznej on 02/03/2017 17:06:29.

5 mW and 4 × 80 seconds acquisition time were applied. Each SERS spectrum for healthy and fungal infected skin samples was averaged from 10 different spots on one sample.

The SEM measurements of *A. flavus* and *T. rubrum* on the SERS substrate (see ESI†) were performed using a FEI Nova™NanoSEM 450 scanning electron microscope with an accelerating voltage of 10 kV under high vacuum conditions.

2.3. SERS substrates

SERS platforms. AgNPs/FTO were prepared according to the patent application P-408785. The substrates were obtained in a three-electrode electrochemical process lasting 15 minutes. Silver nanoparticles (AgNPs) were deposited on an FTO electrode at a constant potential of −1.0 V from an aqueous solution of 0.3 mM $AgNO_3$ and 2.6 mM trisodium citrate dihydrate. All processes were maintained under controlled conditions of temperature and stirring. At the end the SERS substrates were rinsed with deionized water and dried under a stream of air. The sensitivity, reproducibility and stability of the obtained AgNPs/FTO platform were described in the ESI.†

2.4. Fungi culture and SERS sample preparation

The fungi were cultured on sabouraud dextrose agar (SDA; Biocorp, Poland) in Petri dishes held for up to 3 weeks, depending on the species and until colonies were clearly visible, at either 37 °C (*C. krusei*), 30 °C (*T. rubrum*) or 25 °C (*A. flavus*, *S. brumptii*). Afterwards, randomly picked colonies were suspended in 100 μL of 0.9% NaCl solution and homogenized in a microtube with pellet pestle rods with a motor to obtain fragmented hyphae. Then the samples were centrifuged for 5 min at 13 000 rpm at room temperature. Finally, the supernatant fluid was discarded and the pellet of hyphal debris was resuspended in 20 μL of 0.9% NaCl solution. Centrifugation was repeated 5 times to obtain a solution of clean fungal cells. After sample preparation *ca.* 5 μL of aqueous fungal solution was applied to the SERS substrate and the spectra were recorded for at least 30 different spots.

2.5. Collection of skin samples

Skin scrapings were collected from a healthy individual (control) and a patient presenting tinea infection with *T. rubrum*, both being outpatients of the dermatological clinic at the Wrocław Medical University, Wrocław, Poland.

Scrapings were taken from under the nails. Each specimen was placed in a sterile Petri dish and subjected to routine mycological microscopy and culture. The same material was suspended in 20 μL of 0.9% NaCl solution, homogenized and centrifuged for 5 min at 13 000 rpm at room temperature. After sample preparation *ca.* 5 μL of obtained solution was applied to the SERS substrate. In the SERS experiment a total of 20 samples from one healthy and two *T. rubrum* infected human skin samples were analyzed. Each SERS spectrum was averaged from 10 different spots on one sample.

Sampling of the patients was performed under the regulations of the Ethics Committee of the Wrocław Medical University, Wrocław, Poland.

2.6. Chemometric analysis

PCA was applied for all collected spectra of four species of fungal pathogens under the study. This analysis enables us to investigate the spectral variations and to find the most significant contributions to the variance accounted for the PCS. The PCA was performed over the pre-processed Raman spectra in order to (i) evaluate the spectral differences between the fungal species (ii) identify the individual fungal species and (iii) develop a model for the identification of fungal pathogens from clinical samples.

3. Results and discussion

3.1. SERS investigation of spectral changes of fungi

In the presented study the SERS technique was employed for the detection and identification of four fungal pathogenic species namely *S. brumptii*, *A. flavus*, *T. rubrum*, and *C. krusei* on AgNPs/FTO platforms. These platforms exhibit high sensitivity (enhancement factor = 9.0 × 10^6), reproducibility (RSD = 4%) and stability (1.5 month) of the recorded SERS signals (see ESI†). Both biochemical and genetic speciation assays are often laborious, technically demanding, and not always producing consistent results. SERS spectroscopy has been used for the rapid identification of fungi grown on a conventional mycological medium (*i.e.* SDA). It was also used to detect fungi in human skin samples. Here, the time-consuming culture step was omitted. Additionally, we have performed the Raman measurements for major components of the fungal cell walls, *i.e.* chitin, galactomannan, and 1,3-β-glucan. The SERS spectra of the four examined fungal pathogens, in the form of aqueous

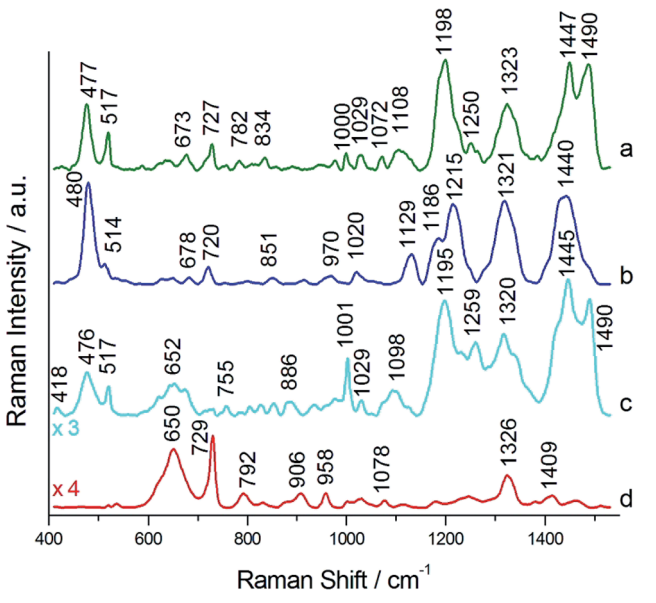

Fig. 1 The average SERS spectra of (a) *S. brumptii*, (b) *A. flavus*, (c) *T. rubrum*, (d) *C. krusei* deposited from aqueous fungal cell solutions onto the SERS platform. Experimental conditions: 5 mW, 785 nm excitation, 3 × 20 seconds acquisition time. The SERS spectra have been baseline-corrected, normalized and shifted vertically for better visualization. Each SERS spectrum was averaged from 30 measurements at different places of the SERS platform.

Published on 15 November 2016. Downloaded by Polska Akademia Nauk Instytut Chemii Fizycznej on 02/03/2017 17:06:29.

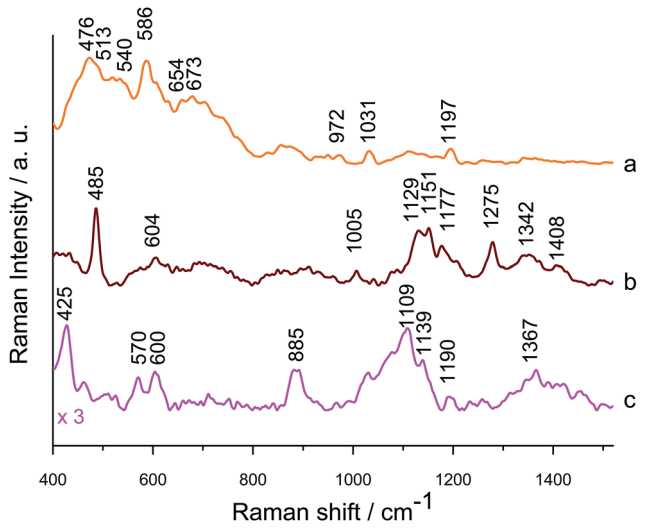

Fig. 2 The average Raman spectra of (a) chitin, (b) galactomannan and (c) 1,3-β-glucan powders. Experimental conditions: 5 mW, 785 nm excitation, 4 × 80 seconds acquisition time. The SERS spectra were baseline-corrected, normalized, and shifted vertically for better visualization. Each average spectrum was obtained from averaging of 30 spectra of each sample.

solutions of clean fungal cells, deposited on SERS-active substrates, are shown in Fig. 1.

For *S. brumptii* (Fig. 1a) several characteristic bands at *ca.* 477, 517, 673, 727, 1000, 1029, 1072, 1108, 1198, 1250, 1323, 1447 and 1490 cm^{-1} are observed. Some of these bands are detected also for compounds constituting the fungal cell wall (Fig. 2).

For instance, bands at *ca.* 673, 1031, and 1197 cm^{-1} are observed in the Raman spectrum of chitin (Fig. 2a). However, the band at *ca.* 1030 cm^{-1} can be also assigned to C–C stretching in carbohydrates and phospholipids.[30] The band at 476 cm^{-1} could be probably assigned to galactomannan or/and chitin, 1000 cm^{-1} to galactomannan, and the band at 1108 cm^{-1} to 1,3-β-glucan (see Fig. 2). In turn, bands at 727 and 1323 cm^{-1} are assigned to the adenine part of flavin adenine dinucleotide (FAD)[31] and amide III, respectively, and the band at *ca.* 1450 cm^{-1} to CH_2 deformation.

In the case of *A. flavus* (Fig. 1b) except for the bands assigned to galactomannan or/and chitin at 482 cm^{-1}, FAD at 720, amide III at 1321 cm^{-1}, and CH_2 deformation at 1440 cm^{-1}, we can also observe small bands at 514 and 970 cm^{-1} which probably come from chitin. The band at 1129 cm^{-1} could be assigned to galactomannan or phospholipids.

The SERS spectrum of *T. rubrum* (Fig. 1c) reveals bands at 418 and 886 cm^{-1}, probably from 1,3-β-glucan, at 517, 1029, 1195 cm^{-1} from chitin, at 1001 cm^{-1} from galactomannan, and at 480 cm^{-1} from galactomannan or/and chitin. We can also observe bands assigned to guanine or tyrosine, amide III, and CH_2 deformation.

Candida krusei (Fig. 1d) exhibits the most distinctive SERS spectrum compared with other fungi, and is very similar to that of bacterial cells. We can observe strong bands at 650 cm^{-1} which derive from guanine or tyrosine[32] at 730 (FAD) and at 1326 cm^{-1} (amide III). The spectrum reveals also a band at

Table 1 Major spectral bands observed in *T. rubrum*, *C. krusei*, *S. brumptii*, and *A. flavus*[a]

Assignment	Range	*S. brumptii*	*A. flavus*	*T. rubrum*	*C. krusei*
1,3-β-Glucan	~420	—	—	+	—
Galactomannan, chitin	475–490	++	++	+	—
Chitin	510–520	+	+	+	—
Guanine, tyrosine	640–675	—	—	+	++
Adenine, glycoside	713–740	+	+	—	++
Cytosine, uracil	745–790	+	—	—	+
C=C deformation, C–N stretching	930–990	—	+	—	+
Phenylalanine, galactomannan, C–C aromatic ring stretching	1000–1010	+	—	+	—
C–C stretching (phospholipids carbohydrates, *e.g.* chitin), C–N stretching	1022–1060	+	—	+	—
O–P–O (DNA), C–C or C–O–C stretching (carbohydrates, *e.g.* 1,3-β-glucan)	1078–1110	+	—	+	+
=C–O–C= (unsaturated fatty acids in lipids), galactomannan	1129–1145	—	+	—	—
C–O ring, aromatic aminoacids in proteins	1150–1186	—	+	—	—
Chitin	1195–1200	++	—	++	—
Amide III (random), thymine	1215–1295	+	++	+	—
Amide III (protein), C–H deformation	1315–1325	++	++	+	—
Adenine, guanine, CH deformation	1330–1345	—	—	—	+
Galactomannan	~1410	—	—	—	+
CH_2 deformation	1440–1475	++	++	++	—
C=C stretching	~1490	++	—	++	—

[a] ++: strong, +: present, —: absent.

This journal is © The Royal Society of Chemistry 2016

Published on 15 November 2016. Downloaded by Polska Akademia Nauk Instytut Chemii Fizycznej on 02/03/2017 17:06:29.

790 cm^{-1} which can be assigned to cytosine or uracil[32] and a band at 958 cm^{-1} which can be linked to C=C deformation. There is only one band at 1409 cm^{-1} that can be assigned to a fungal cell wall component: galactomannan.

To summarize, each spectrum of fungal pathogen has its individual spectral characteristics, creating a species-specific fingerprint. All of the spectral bands observed, and their assignment, for different fungal species are included in Table 1.

The reproducibility of the recorded fungal SERS signals is a crucial parameter for further analytical and biomedical applications of this technique. Therefore, the reproducibility of the SERS signals of *S. brumptii*, *A. flavus*, *T. rubrum*, and *C. krusei* was calculated and is presented in the ESI.† Fig. 3S† shows an example of SERS spectra of *A. flavus*, recorded from different spots within the same sample. To obtain statistically valid results, the strong signal at 485 cm^{-1} was chosen to calculate the average standard deviation (Av. STD). The Av. STD of the intensity of this vibration in the 30 SERS spectra recorded for the same platform is 12%. The reproducibilities of the SERS signals of each studied fungal cell are presented in Table 1S (ESI†).

3.2. Statistical classification

Initially, the PCA analysis was performed in the whole spectral region between 500 and 1600 cm^{-1} for all examined fungal pathogens: *T. rubrum*, *C. krusei*, *S. brumptii*, and *A. flavus*. In the first step we found that the three principal components (PCs) (PC-1, PC-2, and PC-3) are the most diagnostically significant and explain 79%, 17%, and 2% of the variance in the analyzed dataset (Fig. 3a). The differences among the four fungi are due to the bands analyzed in detail in Section 3.1, and are clearly illustrated by loadings plots presented in Fig. 3b. The loading provides information on the variables (wavenumber of the spectrum) that are important for group separation. The loadings plot of PC-1 in Fig. 3b calculated for these four fungi indicates the most important diagnostic variables in the analyzed dataset. Variables with high loading values are the most important for diagnostic purposes. Unlike the SERS spectrum, the loading spectrum contains positive and negative bands, and their corresponding frequencies can be correlated with some of the major variations in the molecular structure of the analyzed fungal pathogens. On the basis of the SERS spectra analysis and loadings plots from PC-1 the most important variation among these four fungi: *T. rubrum*, *C. krusei*, *S. brumptii*, and *A. flavus* was found to be associated with the bands at 476, 520, 1206, 1320 and 1449 cm^{-1} corresponding mainly to the compounds of fungal cell walls *e.g.* 1,3-β-glucan, galactomannan, and chitin (see Fig. 1 and Table 1).

As mentioned above, the PCA analysis performed for these fungi in the whole fingerprint area explains 97% of the variance

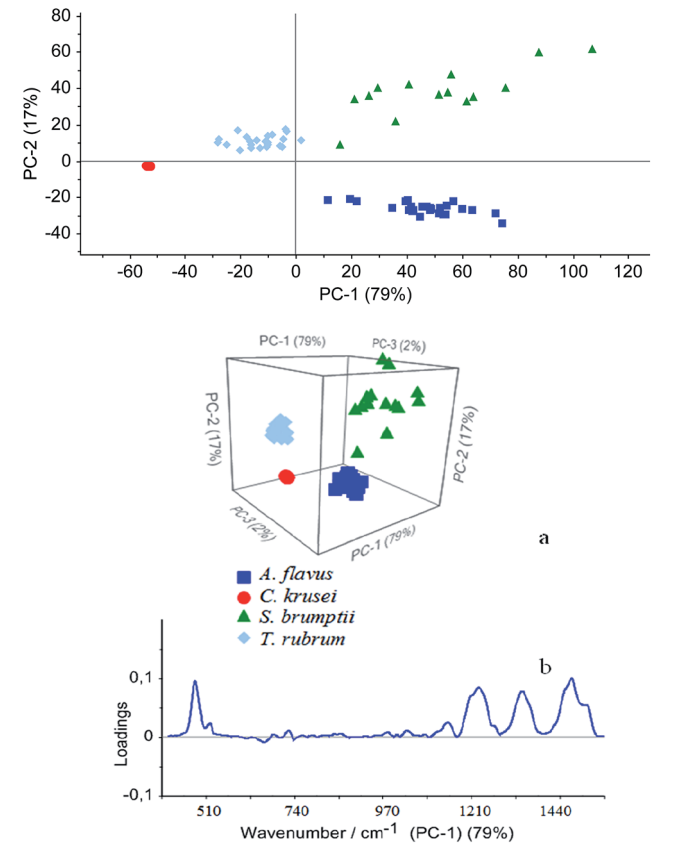

Fig. 3 (a) First three PCs (PC-1, PC-2, and PC-3) scores plot of 3D-PCA calculated for the whole region (500–1600 cm^{-1}) and (b) loadings plot of the PC-1 highlighting regions associated with large loadings for this region, 500–1650 cm^{-1}.

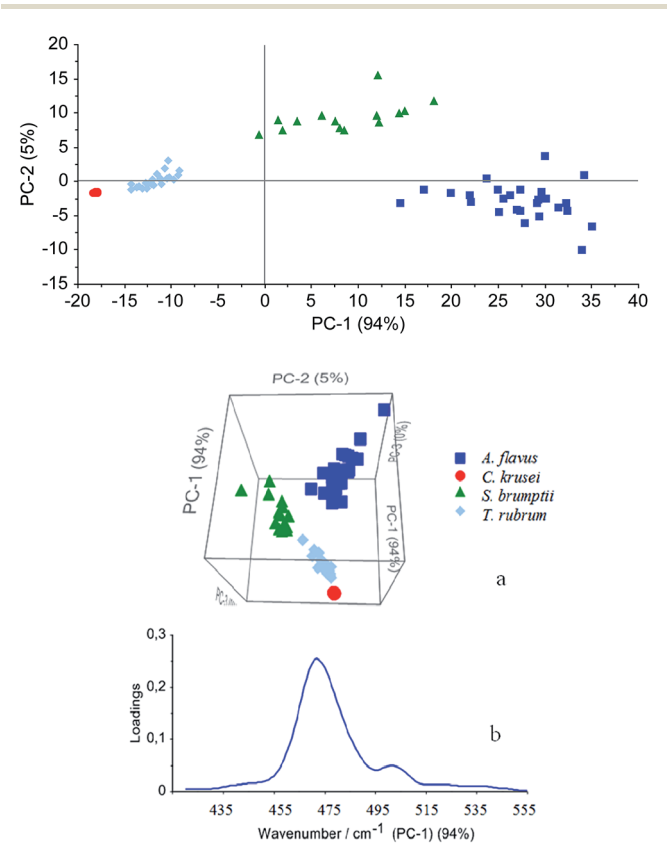

Fig. 4 (a) First three PCs (PC-1, PC-2, and PC-3) scores plot of 3D-PCA calculated for a narrow range (420–560 cm^{-1}) and (b) loadings plot of the first principal component showing the most prominent marker band at 475 cm^{-1}.

Published on 15 November 2016. Downloaded by Polska Akademia Nauk Instytut Chemii Fizycznej on 02/03/2017 17:06:29.

in the data (Fig. 3a). Additionally, for the better classification among the four groups of the analyzed samples the PCA analysis was performed for a selected narrow region (420–560 cm^{-1}) where one of the most prominent marker bands at *ca.* 480 cm^{-1} is present (Fig. 4b). The PCA scores calculated for the region of the chosen marker gave equal PC-1 and PC-2 values of 98% of total variance (see Fig. 4a). This demonstrates the excellent separation of the studied human fungal pathogens into four separated clusters corresponding to the *T. rubrum*, *C. krusei*, *S. brumptii*, and *A. flavus*, respectively (Fig. 4a).

3.3. Identification of fungal pathogens from clinical skin samples

The purpose of this study was also to determine the effectiveness of SERS and PCA analysis in the identification of fungal pathogens from clinical skin samples. Fig. 5a and b show the SERS spectra of aqueous solutions of the homogenized skin samples recovered from a healthy subject (without any mycotic disease) and a patient with *T. rubrum* infection of nails (onychomycosis). The SERS spectra from healthy skin (Fig. 5a) present contributions from the main components of biological tissues: proteins, lipids, nucleic acids, carbohydrates, and especially collagen. The most intense bands are located at 1446, 1351, 1275, 1049, 1027, 1001, 850, and 637 cm^{-1}. The SERS spectra from healthy skin were similar to those reported by other research groups, obtained from human and animal species for both *in vivo* or *ex vivo* measurements.[33–35] The vibrational modes seen in the high wavenumber region of this spectrum, such as the 1446 cm^{-1}, are assigned to nucleic acid constituents and proteins CH_3 bending vibrations. The 1360–1280 cm^{-1} spectral range exhibits an intense broad band centered at 1356 cm^{-1}. This Raman mode is assigned to phospholipids. This broad band contains other contributions as well; the band located at 1316 cm^{-1} is assigned to nucleic acids and collagen and that at 1331 cm^{-1} is assigned to the bending mode of collagen and lipids.[36,37] The 1030–1130 cm^{-1} spectral range presents useful information on the nature of the stratum corneum lipid bilayer packing.[38] The C–C stretching modes of lipids are observed at 1085 cm^{-1} and 1048 cm^{-1}. The main band of the phenylalanine of collagen appears at 1001 cm^{-1} and 1027 cm^{-1}.[39] The 853 cm^{-1} band is typical for collagen due to the proline/hydroxyproline vibration and the C–C stretching vibrations in the protein structure. In the low wavenumber region of the spectra more nucleic acid bands can be observed, such as the 637 cm^{-1} band which may be assigned to a superposition of a tyrosine vibration and the guanine SERS fingerprint, or the 725 cm^{-1} assigned to adenine.[40] The SERS spectrum recorded from *T. rubrum* infected skin samples (Fig. 5b) exhibits a lot of intense bands in the same spectral ranges as the spectrum of a control sample (healthy skin) (Fig. 5a). However, a detailed analysis of SERS spectra of *T. rubrum* infected skin reveals remarkable differences. We can observe new SERS bands at 476, 616, 675, 831, 953, 1197 and 1319 cm^{-1} which correspond to *T. rubrum* vibrations (Fig. 1c and Table 1) and clearly indicate the presence of *T. rubrum* fungus in the examined skin.

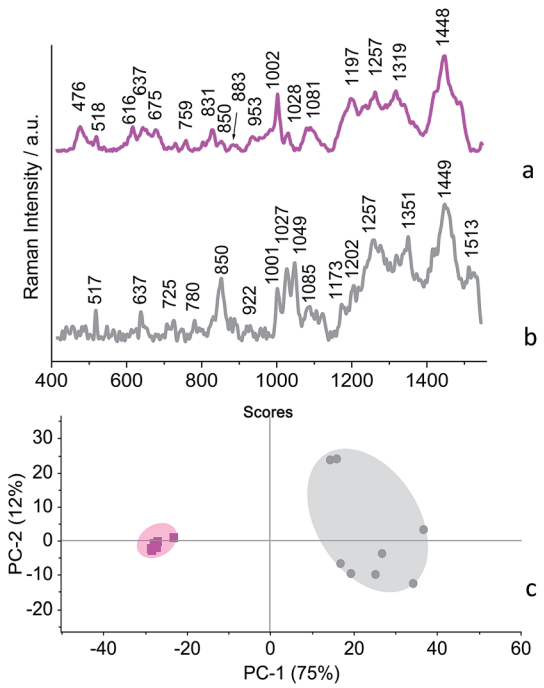

Fig. 5 SERS spectra of aqueous solutions of homogenized skin samples derived from a healthy subject (a) and a patient infected with *T. rubrum* (b), deposited onto the SERS platform. Experimental conditions: 5 mW, 785 nm excitation, 4 × 80 seconds acquisition time. The SERS spectra were baseline-corrected, normalized and shifted vertically for better visualization. Each SERS spectrum was averaged from 10 different spots on one sample. PCA scores of the first two principal components PC-1 (95% of the total variance) and PC-2 (2% of the total variance) showing the comparison between the healthy and *T. rubrum* infected skin samples for the 500–1650 cm^{-1} range (c).

Moreover, in order to improve the differentiation between healthy and infected human skin, PCA analysis was applied. Fig. 5b displays the scores plot of the first two principal components PC-1 (75% of the total variance) and PC-2 (12% of the total variance) of the healthy and *T. rubrum* infected skin samples for the whole wavenumber region 500–1600 cm^{-1}. Fig. 6S (see ESI†) displays the loadings plots of PC-1 calculated for this region. By analysing these plots one can indicate the most important diagnostic variables in the analyzed dataset (*e.g.* 675, 850, 953, 1200 and 1319, 1445 cm^{-1}), which reflect the characteristic bands in the *T. rubrum* SERS spectrum and demonstrate the ability of the SERS method to identify individual fungal pathogens in clinical skin samples.

The variations observed in Fig. 5c (gray cluster) among the calculated scores for the infected samples are rather natural. Each patient is in a different stage of infection, which results in a different number of the fungal species present on the skin sample. Additionally, each patient has a different response of the immune systems, and thus also the final SERS spectrum will be different. The obtained scores are nicely grouped in two clusters: scores of the healthy skin samples are focused in a very tiny area, while, as was explained above, the scores of the infected skin samples are more spread out. Moreover, it should be highlighted that these two clusters are separated by a big distance – around 40 (in absolute values). This distance

 This journal is © The Royal Society of Chemistry 2016

Published on 15 November 2016. Downloaded by Polska Akademia Nauk Instytut Chemii Fizycznej on 02/03/2017 17:06:29.

indicates that the studied samples are really different and are nicely grouped/classified using the proposed PCA model.

4. Conclusions

SERS spectroscopy coupled with PCA analysis seems to provide an attractive approach for discrimination between fungal pathogens in humans with high accuracy. In this study it allowed label-free, simultaneous, and rapid identification of four important human fungal pathogenic species, *i.e. T. rubrum*, *C. krusei*, *S. brumptii*, and *A. flavus*. Additionally, we were able to detect and identify *T. rubrum* directly in the clinical material (skin samples). We used PCA to visualize fungi differentiation in the three-dimensional space defined by PC-1, PC-2 and PC- 3. PCA calculations were used to demonstrate the impact of the novel SERS strategy for fungi identification with 98% accuracy. The results obtained in this study demonstrate that SERS is a powerful technique for the detection and identification of pathogenic fungi. The development of such a rapid and effective method of identification of pathogenic fungi would greatly facilitate the diagnosis and therefore would allow the start of the appropriate medical treatments. However, further research and validation with other types of samples and fungal species are needed before SERS can become a robust tool for pathogen identification.

Acknowledgements

The authors would like to thank Monika Księżopolska-Gocalska and Paweł Albrycht for SERS substrate preparation. These studies were supported by the NCBiR under grant PBS2/A1/8/2013.

References

1 D. L. Hawksworth, The magnitude of fungal diversity: the 1.5 million species estimate revisited, *Mycol. Res.*, 2001, **105**, 1422–1432.
2 L. H. Taylor, S. M. Latham and M. E. J. Woolhouse, Risk factors for human disease emergence, *Philos. Trans. R. Soc. London, Ser. B*, 2001, **356**, 983–989.
3 J. W. Badley, T. P. Stroud, D. Salzman and P. G. Pappas, Invasive mold infections in allogeneic bone marrow transplant recipients, *Clin. Infect. Dis.*, 2001, **32**, 1319–1324.
4 T. A. Clark and R. A. Hajjeh, Recent trends in the epidemiology of invasive mycoses, *Curr. Opin. Infect. Dis.*, 2002, **15**, 569–574.
5 B. Willinger, Laboratory diagnosis and therapy of invasive fungal infections, *Curr. Drug Targets*, 2006, **7**, 513–522.
6 P. P. Bosshard, Incubation of fungal cultures: Wiad. Parazytol. how long is long enough?, *Mycoses*, 2011, **54**, 539–545.
7 A. Kurnatowska and P. Kurnatowski, The diagnostic methods applied in mycology, *Wiad. Parazytol.*, 2008, **54**, 177–185.
8 D. A. Stevens, Diagnosis of fungal infections: current status, *J. Antimicrob. Chemother.*, 2002, **49**, 11–19.
9 G. S. Sandhu, B. C. Kline, L. Stockman and G. D. Roberts, Molecular Probes for Diagnosis of Fungal Infections, *J. Clin. Microbiol.*, 1995, **33**, 2913–2919.
10 J. A. Van Burik, D. Myerson, R. W. Schreckhire and R. A. Bowden, Panfungal PCR assay for detection of fungal infection in human blood specimens, *J. Clin. Microbiol.*, 1998, **36**, 1169–1175.
11 M. Fleischmann, P. J. Hendra and A. J. McQuillan, Raman spectra of pyridine adsorbed at a silver electrode, *Chem. Phys. Lett.*, 1974, **26**, 163–166.
12 M. A. Prusinkiewicz, F. Farazkhorasani, J. J. Dynes, J. Wang, K. M. Gough and S. G. Kaminskyj, Proof-of-principle for SERS imaging of Aspergillus nidulans hyphae using *in vivo* synthesis of gold nanoparticles, *Analyst*, 2012, **137**, 4934–4942.
13 A. Szeghalmi, S. G. Kaminskyj, P. Rosch, J. Popp and K. M. Gough, Time fluctuations and imaging in the SERS spectra of fungal hypha grown on nanostructured substrates, *J. Phys. Chem. B*, 2007, **111**, 12916–12924.
14 A. Sivanesan, E. Witkowska, W. Adamkiewicz, L. Dziewit, A. Kaminska and J. Waluk, Nanostructured silver–gold bimetallic SERS substrates for selective identification of bacteria in human blood, *Analyst*, 2014, **139**, 1037–1043.
15 T. Szymborski, E. Witkowska, W. Adamkiewicz, J. Waluk and A. Kaminska, Electrospun polymer mat as a SERS platform for the immobilization and detection of bacteria from fluids, *Analyst*, 2015, **139**, 5061–5064.
16 H. Zhou, D. Yang, N. P. Ivleva, N. E. Mircescu, R. Niessner and C. Haisch, SERS detection of bacteria in water by *in situ* coating with Ag nanoparticles, *Anal. Chem.*, 2014, **86**, 1525–1533.
17 S. Efrima and L. Zeiri, Understanding SERS of bacteria, *J. Raman Spectrosc.*, 2009, **40**, 277–288.
18 K. Gracie, E. Correa, S. Mabbott, J. A. Dougan, D. Graham, R. Goodacre and K. Faulds, Simultaneous detection and quantification of three bacterial meningitis pathogens by SERS, *Chem. Sci.*, 2014, **5**, 1030–1040.
19 A. Kaminska, E. Witkowska, K. Winkler, I. Dzięcielewski, J. L. Weyher and J. Waluk, Detection of Hepatitis B virus antigen from human blood: SERS immunoassay in a microfluidic system, *Biosens. Bioelectron.*, 2015, **66**, 461–467.
20 N. R. Isola, D. L. Stokes and T. Vo-Dinh, Surface-Enhanced Raman Gene Probe for HIV Detection, *Anal. Chem.*, 1998, **70**, 1352–1356.
21 M. T. Hedayati, A. C. Pasqualotto, P. A. Warn, P. Bowyer and D. W. Denning, Aspergillus flavus: human pathogen, allergen and mycotoxin producer, *Microbiology*, 2007, **153**, 1677–1692.
22 N. Zaias and G. Rebell, Chronic dermatophytosis caused by Trichophyton rubrum, *Dermatology*, 1996, **35**, S17–S20.
23 J. Naidu, S. M. Singh and M. Pouranik, Onychomycosis caused by Scopulariopsis brumptii. A case report and sensitivity studies, *Mycopathologia*, 1991, **113**, 159–164.
24 R. Patel, C. A. Gustaferro, R. A. Krom, R. H. Wiesner, G. D. Roberts and C. V. Paya, Phaeohyphomycosis due to

Published on 15 November 2016. Downloaded by Polska Akademia Nauk Instytut Chemii Fizycznej on 02/03/2017 17:06:29.

Scopulariopsis brumptii in a liver transplant recipient, *Clin. Infect. Dis.*, 1994, **19**, 198–200.

25 E. M. Shankar, R. Vignesh, R. C. Barton, P. Balakrishnan, K. G. Murugavel, V. Velu, H. Kownhar, C. A. Lloyd, S. Solomon, U. A. Rao and N. Kumarasamy, Hydrothorax in association with Scopulariopsis brumptii in an AIDS patient in Chennai, India, *Trans. R. Soc. Trop. Med. Hyg.*, 2007, **101**, 1270–1272.

26 D. A. Persons, M. Laughlin, D. Tanner, J. Perfect, J. P. Gockerman and J. W. Hathorn, Fluconazole and Candida krusei fungemia, *N. Engl. J. Med.*, 1991, **325**, 1315.

27 P. L. Stiles, J. A. Dieringer, N. C. Shah and R. P. Van Duyne, Surface-enhanced Raman Spectroscopy, *Annu. Rev. Anal. Chem.*, 2008, **1**, 601–626.

28 B. Sharma, R. R. Frontiera, A. I. Henry, E. Ringe and R. P. Van Duyne, *Mater. Today*, 2012, **15**, 16–25.

29 S. M. Bowman and S. J. Free, The structure and synthesis of the fungal cell wall, *BioEssays*, 2006, **28**, 799–808.

30 M. C. Demirel, P. Kao, N. Malvadkar, H. Wang, M. Poss and D. L. Allara, Bio-Organism Sensing *via* Surface Enhanced Raman Spectroscopy on Controlled Metal/Polymer Nanostructured Substrates, *Biointerphases*, 2009, **4**, 35–41.

31 C. Fan, Z. Hu, A. Mustapha and M. Lin, Rapid detection of food- and waterborne bacteria using surface-enhanced Raman spectroscopy coupled with silver nanosubstrates, *Appl. Microbiol. Biotechnol.*, 2011, **92**, 1053–1061.

32 T. Luna-Pineda, K. Soto-Feliciano, E. De la Cruz-Montoya, L. C. P. Londono, C. Rios-Velazquez and S. P. Hernandez-Rivera, Spectroscopic characterization of biological agents using FTIR, normal Raman and surface-enhanced Raman spectroscopies, in *Chemical and Biological Sensing VIII*, ed. A. W. Fountain, Proceedings of SPIE – The International Society of Optical Engineering, Bellingham, 2007, pp. 65540K1–65540K11.

33 M. Gniadecka, P. A. Philipsen, S. Sigurdsson, S. Wessel, O. F. Nielsen, D. H. Christensen, J. Hercogova, K. Rossen, H. K. Thomsen, R. Gniadecki, L. Kai Hansen and H. C. Wulf, Melanoma Diagnosis by Raman Spectroscopy and Neural Networks: Structure Alterations in Proteins and Lipids in Intact Cancer Tissue, *J. Invest. Dermatol.*, 2004, **122**, 443–449.

34 H. Wang, N. Huang, J. Zhao, H. Lui, M. Korbelika and H. Zeng, Depth-resolved *in vivo* micro-Raman spectroscopy of a murine skin tumor model reveals cancer-specific spectral biomarkers, *J. Raman Spectrosc.*, 2011, **42**, 160–166.

35 J. Zhao, H. Lui, D. McLean and H. Zeng, Real-Time Raman Spectroscopy for Noninvasive *in vivo* Skin Analysis and Diagnosis, in *New Developmenst in Biomedical Engineering*, ed. D. Campolo, InTech, 2010, pp. 455–475.

36 J. Kneipp, H. Kneipp, B. Witting and K. Kneipp, Novel optical nanosensors for probing and imaging live cells, *Nanomedicine*, 2010, **6**, 214–226.

37 O. Aydin, M. Kahraman, E. Kilic and M. Culha, Surface-enhanced Raman scattering of rat tissues, *Appl. Spectrosc.*, 2009, **63**, 662–668.

38 B. W. Barry, H. G. M. Edwards and A. C. Williams, Fourier transform Raman and infrared vibrational study of human skin: assignment of spectral bands, *J. Raman Spectrosc.*, 1992, **23**, 641–645.

39 S. Fendel and B. Schrader, Investigation of skin and skin lesions by NIR-FT-Raman spectroscopy, *Fresenius' J. Anal. Chem.*, 1998, **360**, 609–613.

40 A. Raj, K. Raju, H. T. Varghese, C. M. Granadeiro, H. I. S. Nogueirad and C. Y. Panicker, IR, Raman and SERS Spectra of 2-(Methoxycarbonylmethylsulfanyl)-3,5-dinitrobenzene Carboxylic Acid, *J. Braz. Chem. Soc.*, 2009, **20**, 549–559.

 This journal is © The Royal Society of Chemistry 2016